Astrocyte Process Growth Induction by Actin Breakdown

David M. Baorto, Wilfredo Mellado, and Michael L. Shelanski

Department of Pathology and Center for Neurobiology and Behavior, College of Physicians and Surgeons of Columbia University, New York, New York 10032

Abstract. cAMP analogues such as dibutyryl cAMP (dBcAMP) have been shown to induce the formation of processes in cultured primary astrocytes. We observe that the processes form by elongation as well as the previously reported retraction of cytoplasm around cytoskeletal elements. The most prominent cytoskeletal change that occurs in response to dBcAMP is a rearrangement of actin filaments characterized by a loss of cortical F-actin staining and the appearance of actin filament staining at the tips of the processes. If cortical actin filaments are disrupted with dihydrocytochalasin B, processes form that are similar to those induced by dBcAMP suggesting that the disruption of the cortical actin network is the pivotal step in process formation. Reorganization of the actin filament network in response to cAMP is accompanied by a decrease in phosphate incorporation into the regulatory light chain of myosin (MLC). Two selective inhibitors of MLC kinase (MLCK), ML-9 and KT5926, as well as a calmodulin antagonist (W7), which would also inhibit MLCK activation, all induce astrocytic process growth implicating MLCK as a control point in process initiation. We also found that dBcAMP and ML-9 both cause a decrease in the phosphate content of actin depolymerizing factor, suggesting that this protein and myosin light chain are the effectors of actin cytoskeleton reorganization and process growth.

ASTROCYTES in vivo have multiple elongated processes. While the functions of astrocytes are not completely understood, it is likely that their shape is critical to many of them. For example, astrocytes are known to buffer potassium ions released from neuronal membranes and to take up transmitters released from neuronal synapses (Walz, 1989; Kimelberg and Norenberg, 1989). These roles are aided by the high surface area to volume ratio that is provided by multiple thin processes. The recent finding that waves of calcium ions can propagate between astrocytes has suggested that astrocyte processes may carry long-range signals within the brain (Cornell-Bell et al., 1990).

Astrocytes prepared from neonatal cerebral hemispheres or cerebella and cultured in serum-containing medium are polygonal and have no processes at low density. However, they can undergo dramatic shape changes in tissue culture resulting in forms similar to their in vivo morphology when treated with either live neurons (Hatten, 1985) or cAMP analogues such as dibutyryl cAMP (dBcAMP)[1] (Lim et al., 1973; Trimmer et al., 1982; Goldman and Chiu, 1984). While neuronal contact has been reported to cause astrocyte processes to elongate from a contracted cell body (Mason et al., 1988), short term treatment with cAMP analogues has been reported to result in process formation by retraction of spread cytoplasm around organized cytoskeletal elements (Goldman and Abramson, 1990). We find that dBcAMP treatment of spread astrocytes also results in slow elongation of the processes left behind by retraction, and that astrocytes plated in the presence of dBcAMP extend processes from a contracted cell body without prior spreading.

Little is known about the machinery that results in this dramatic shape change. We investigated the role of cytoskeletal components in the growth of cerebellar astrocytic processes in tissue culture. Our observations reveal a rearrangement of actin filaments upon treatment with dBcAMP that is characterized by a disruption of actin filaments of the cell cortex, accompanied by the appearance of actin filament staining at the tips of the growing processes. The previous observation of stress fiber disruption in dBcAMP-treated astrocytes (Goldman and Abramson, 1990) supports the idea that the actin filament system is a target of cAMP in astrocytes.

Materials and Methods

Astrocyte Preparation and Culture

Astrocytes were prepared from the cerebella of 4-d-old Sprague Dawley rats by modifying the method of Hatten (1985). Whole cerebella were dissected from two litters (18–24 rats), washed in a PBS solution without calcium or magnesium, and incubated for 3 min in PBS containing 1.5 mg/ml of $MgSO_4$-$7H_2O$ solution, 1.5 mg/ml trypsin (1:250, Difco Laboratories, Detroit, MI) and 0.15 mg/ml DNase I (Worthington Biochemical Corporation, Freehold, New Jersey). The cerebella were then placed into a petri dish containing fresh PBS, and dissected free of the meninges. They were

1. *Abbreviations used in this paper*: ADF, actin depolymerizing factor; dBcAMP, dibutyryl cAMP; MLC, myosin light chain; MLCK, MLC kinase.

placed in a sterile tube containing 3 ml of a 1:1 mixture of DME and Ham's F12 medium (Gibco Laboratories, Grand Island, NY) plus 0.5 mg/ml of DNase I. The tissue was broken up by triturating 10 times through a normal bore, fire-polished Pasteur pipet, then again 10 times through a smaller bore, fire-polished Pasteur pipet (about half the diameter of normal bore). The cell suspension was passed through a 33-μm mesh size Nitex membrane, then pelleted by centrifugation for 5 min at 1,000 rpm. The pellet was resuspended in fresh medium plus 0.15 mg/ml of DNase I in a volume of 1 ml for every four cerebella. Each ml was layered onto 10 ml of 35% Percoll (in PBS, pH 7.4, plus 2 mM EDTA) in a 50-ml conical tube and centrifuged at 3,000 rpm for 10 min (using slow acceleration and deceleration to preserve the step gradient). The interface between medium and Percoll was harvested with an 18-gauge needle on a 10-ml syringe, diluted with a 10-fold excess of PBS, and the cells were pelleted at 1,000 rpm for 5 min.

This astrocyte enriched fraction was further purified by a differential adhesion step. The pellet was resuspended in a 1:1 mixture of DMEM and F12 plus 10% heat-inactivated horse serum and 5% heat-inactivated calf serum (DF5-10), and plated into 60-mm petri dishes (Falcon Labware, Oxnard, CA) that had been previously incubated for 30 min with 100 μg/ml poly-L-lysine and rinsed with water (one dish for every four cerebella). After 40–60 min the dishes were tapped hard 10–20 times, and the nonadherent cells were discarded. The remaining cells were rinsed once with DF5-10, 3 ml DF5-10 was then added to each dish, and they were placed in the incubator for 4 d. After that they were carried up to 3 wk by splitting them 1:5 once a week into tissue culture dishes not treated with poly-L-lysine.

The silicon rubber substrate was prepared as described by Harris et al. (1980). A 1-mm-thick coating of 30,000 centistokes viscosity polydimethylsiloxane (200 Fluid; Dow Corning Corp., Midland, MI) was spread onto the surface of a 12-mm coverslip. The coverslip was then inverted and passed through a low Bunsen burner flame (~1 s). The coverslip was then placed in a tissue culture dish with the silicon side facing up, and medium was carefully added to prevent the coverslip from floating.

Pharmacological Treatments

Cells were replated at a density of 20% of confluence onto glass coverslips that had been treated for 30 min with poly-L-lysine or onto tissue culture plastic. Drugs were then added either at the time of plating or after the cells had spread. All drugs were obtained from Sigma Chemical Co. (St. Louis, MO) unless otherwise specified. dBcAMP and dBcGMP were used at 1 mM. ML-9 (Seikagaku America, Rockville, MD) was stored as a 10-mM frozen stock in DMSO (anhydrous, Aldrich Chemical Co., Inc., Milwaukee, WI), and used at a final concentration range of 10–100 μM. KT5926 (Kamiya Biomedical Co., Thousand Oaks, CA) was stored as a 2-mM frozen stock in DMSO and used at a final concentration range of 1–25 μM. W-7 was also kept as a 100-mM frozen stock in DMSO and used at a final concentration range of 1–100 μM. Dihydrocytochalasin B was stored as a 5-mg/ml frozen stock in DMSO and used at 5–50 μg/ml final concentration. 8-(4-chlorophenylthio) adenosine 3':5'-cyclic monophosphate (CPT) was used at 250 μM. Forskolin was kept as a frozen stock and used at 100 μM. Isoproterenol was used at 1–10 μM. After treatment the cells were observed and photographed by phase-contrast microscopy. Alternatively, cells on coverslips were fixed for immunostaining or cells in tissue culture dishes were extracted for biochemical experiments.

Fluorescence Staining and EM

Immunofluorescence staining of the cells was conducted according to standard procedures. Rabbit polyclonal antiserum against actin was generously provided by Dr. J. C. Bulinski (Columbia University). IgG fraction of antiserum against platelet myosin was generously provided by Dr. R. Adelstein (National Institutes of Health). Rabbit polyclonal antiserum against the glial fibrillary acidic protein was generously provided by Dr. R. Liem (Columbia University). Coverslips (12-mm diameter, Fischer Scientific Co., Pittsburgh, PA) containing the cells were fixed in 4% paraformaldehyde in PBS for 10 min at room temperature. The cells were then permeabilized by incubating with ice cold methanol for 7 min in the freezer. Alternatively, 1% Triton X 100 was included in the 4% paraformaldehyde solution to reduce staining of soluble actin. After rinsing with PBS, a blocking solution consisting of 10% lamb serum and 10% goat serum in PBS was added for 10 min. The primary antibodies were then added and incubated with the cells for 1 h. The coverslips were then rinsed with PBS, and the secondary antibodies conjugated to either fluorescein or rhodamine were added for 1 h. The coverslips were rinsed and mounted in Aquamount (Lerner Laboratories, Pittsburgh, PA). Rhodamine phalloidin was obtained from Molecular Probes (Eugene, OR) and used according to the manufacturer's suggested protocols.

For EM, cells were fixed with 2.5% glutaraldehyde in PBS for 30 min at room temperature. After washing three times with PBS, the cultures were postfixed in 1% osmium tetroxide for 30 min, and then washed in PBS for 30 min. The cultures were then dehydrated in increasing ethanol concentrations, and embedded, SPI-PON (SPI Supplies Division of Structures Probe, Inc., West Chester, PA). 60–90 nm sections were cut on a Sorvall MT 500 microtome, then stained with uranyl acetate and lead citrate and photographed using a JEOL 100S electron microscope.

Metabolic Labeling

Labeling experiments were done with astrocytes that had been replated into 60-mm tissue culture dishes for 1 d. After one rinse with KRHG (Hepes-buffered Krebs ringer solution containing 25 mM Hepes, pH 7.5, 100 mM NaCl, 4.8 mM KCl, 1.3 mM $CaCl_2$, 1.2 mM $MgSO_4$, 5.6 mM D-glucose), 300–500 μCi of ^{32}P orthophosphate (NEN, Boston, MA) per ml was added in 1.5 ml KRHG plus 1% heat-inactivated calf serum. After a 3-h labeling period at 37°C, drugs were added in the continued presence of label. After the treatment period, the cells were rinsed three times with warm PBS. The cells were then used for immunoprecipitating specific proteins or for obtaining Triton-soluble and -insoluble fractions.

Immunoprecipitation and Extractions

Immunoprecipitation of the myosin complex was done according to Ludowyke et al. (1989). The labeled and treated cells were scraped into 250 μl of lysis buffer consisting of 1% NP-40, 100 mM sodium pyrophosphate, 250 mM sodium chloride, 50 mM sodium fluoride, 5 mM EGTA, 0.1 mM phenylmethylsulfonyl chloride, 15 mM b-mercaptoethanol, and 20 mM Tris-HCl (pH 7.9) (Lysis buffer 1). This lysate was centrifuged at 100,000 *g* for 5 min at 4°C, and the supernatant was incubated with 5 mg protein A-Sepharose beads (Sigma Chemical Company, St. Louis, MO) for 1 h at 4°C, with constant rotating, as a preclearing step. After centrifuging for 2 min to remove the beads, the supernatant was incubated with 10 μl of antiplatelet myosin antibody (IgG fraction) for 2 h at 4°C, with constant rotation. 5 mg protein A-Sepharose was added and incubated at 4°C, rotating for one more hour. The beads were rinsed three times with 200 μl of lysis buffer 1, and 100 μl of sample buffer was added to sample to prepare for gel loading.

Immunoprecipitating antibody against actin depolymerizing factor (ADF) was generously provided by Dr. J. Bamburg (Colorado State University). The procedure used for the immunoprecipitation of ADF was as follows. The labeled and treated cells were scraped into 200 μl of lysis buffer 2, which differs from lysis buffer 1 by the substitution of 1% SDS for 1% NP-40. This was boiled for 5 min, centrifuged at 100,000 *g* for 5 min at 4°C, and 4 vol of lysis 1 buffer were added to the supernatant. The immunoprecipitation was then done as described above, using 20 μl of IgG fraction of antibody against ADF.

To obtain Triton-soluble and -insoluble fractions, the labeled cells were incubated for 7 min in extraction buffer (0.1% Triton × 100, 0.1% MES, pH 6.8, 1.0 mM EGTA, 0.5 mM $MgCl_2$, 2.0 M glycerol, 25 mM NaF, and 1.0 mM phenylmethylsulfonyl fluoride [PMSF]). This was called the Triton soluble fraction. The remaining cellular material was taken up in sample buffer and called the Triton insoluble fraction.

Phosphopeptides were analyzed from immunoprecipitated samples by the method of Nishikawa et al. (1983).

Gel Methods

SDS-PAGE was done according to Laemmli (1970). 12, 15, and 6–12% gradient gels were used. Gels were run 24 h at a constant current of ~6 mA per gel. To visualize proteins, the gels were silver stained according to Wray et al. (1981). For autoradiography, gels were dried overnight at room temperature between two sheets of Biogelwrap membrane (BioDesign Inc., Carmel, NY). They were then exposed to Kodak XAR 5 film using an intensifier screen. Immunoblots (Western blots) were done according to Towbin et al. (1979). The Trans-Blot Cell apparatus (Bio-Rad Laboratories, Richmond, CA) was used, and proteins were transferred at a current of 100 mA for 4 h. Protein size markers were visualized on the nitrocellulose membrane by immersing the membrane in a 2% solution of Ponseau S (Sigma Chemical Co.) in 2% TCA for 5 min, then rinsing well with water. The membrane to be stained with antibody was rocked for 1 h in a blocking solution consisting of 5% powdered milk in PBS. The primary antibody diluted

into the blocking solution was then incubated with the membrane for 1.5 h. The membrane was then washed three times for 10 min with 0.05% Triton X 100 in PBS, and incubated with 1.0 μCi/ml of ^{125}I-protein A (Amersham Corp., Arlington Heights, IL) in 5% BSA and 0.05% Triton X 100 for 1 h at room temperature. It was again washed three times for 10 min in 0.05% Triton X 100 in PBS, dried, and exposed to Kodak XAR 5 film.

Results

How Do Processes Form: Cavitation vs. Elongation

Cultured astrocytes were replated onto Falcon tissue culture plastic dishes at low density. These cells are polygonal and well-spread with no processes (Fig. 1 *a*). Upon treatment with 1 mM dBcAMP, they form processes. Some cells respond as early as 20 min after treatment, with ~75% of the cells responding by 3 h. Goldman and Abramson (1990) have reported that this change in response to dBcAMP occurs by retraction of cytoplasm around organized cytoskeletal elements. While we also observe retraction, we find that the retraction step does not need to occur for the process to grow. This growth is seen as an incremental increase in the length of processes from one frame to the next in the time lapse micrographs (Fig. 1, *a–d*).

Identical morphological transformations are elicited by another cAMP analogue, CPT, as well as by forskolin and isoproterenol, which are known to elevate cAMP in astrocytes (Murphy and Pierce, 1987; McCarthy and de Vellis, 1978; Shain et al., 1987). No morphological change is elicited by dibutyryl cyclic GMP.

A second type of astrocytic process formation is seen when astrocytes are treated with dBcAMP at the time of plating. In this case, the cells attach to the tissue culture plastic in the presence of dBcAMP and processes begin to extend along the substrate from the round cell body. 3 h after the cells adhere in the presence of dBcAMP the processes are similar in both caliber and length to those of cells that have been fully spread before dBcAMP treatment.

Reorganization of Actin Filaments in dBcAMP Induced Process Outgrowth from Cerebellar Astrocytes

In untreated astrocytes actin filaments are seen at the cell cortex appearing to outline the cell border, and in fine stress fibers running linearly across the cell. For the first 16 h after plating, the cortical staining is very prominent and stress fibers are absent. Actin staining in control cells appears as a bright circular ring 3 h after plating (Fig. 2 *a*), which then becomes polygonal as the cell spreads. The cortex is seen by EM as a dense band of filaments (Fig. 2 *c*). Within several hours, and often within 20 min, after dBcAMP treatment there is a loss of the cortical actin ring reflected in a loss of cortical actin staining by immunofluorescence (Fig. 2 *b*) and a large reduction in the number of actin filaments in the cortex (Fig. 2 *d*). Though actin filament staining is no longer prominent in the cortex, distinct actin staining can be seen at the tips of many of the processes (Fig. 2 *b*). Similar results are obtained whether actin antibody or rhodamine phalloidin is used as a probe for actin. The effect on actin filaments is similar when the cells have been allowed to spread before treatment with dBcAMP or when they are treated at the time of plating. Nocodazole (10 μm), a drug that disrupts microtubules by binding to tubulin monomers, prevents the formation of astrocytic processes with dBcAMP, and partially prevents the actin rearrangement. We examined whether the observed morphological disruption of actin filaments resulted in a net disassembly of filaments into soluble actin. Densitometric scanning of autoradiograms from three experiments showed that, under our culture conditions, a 3-h treatment with dBcAMP caused a 15.7 ± 0.5% reduction in the proportion of actin in the Triton-insoluble pool. Total actin remained unchanged.

Disruption of Actin Filaments by Dihydrocytochalasin B Is Sufficient to Cause Astrocyte Process Growth

To test whether the breakdown of cortical actin seen in response to dBcAMP was critical in the formation of processes, astrocytes were treated with 50 μM dihydrocytochalasin B, a treatment that directly disrupts cortical actin filaments. This treatment caused a loss of filamentous actin staining in the cell cortex with only traces of irregular and punctate staining remaining. Interestingly, it also caused a retraction of the cytoplasm leaving elongating processes very similar to those seen with dBcAMP. To isolate the elongation phase, astrocytes were treated with dihydrocytochalasin B at the time of plating. Under these conditions, the cells adhere rapidly to the tissue culture plastic but do not spread. Within 30–90 min several extensions begin to emerge from the cell body, along the tissue culture plastic but not out into the

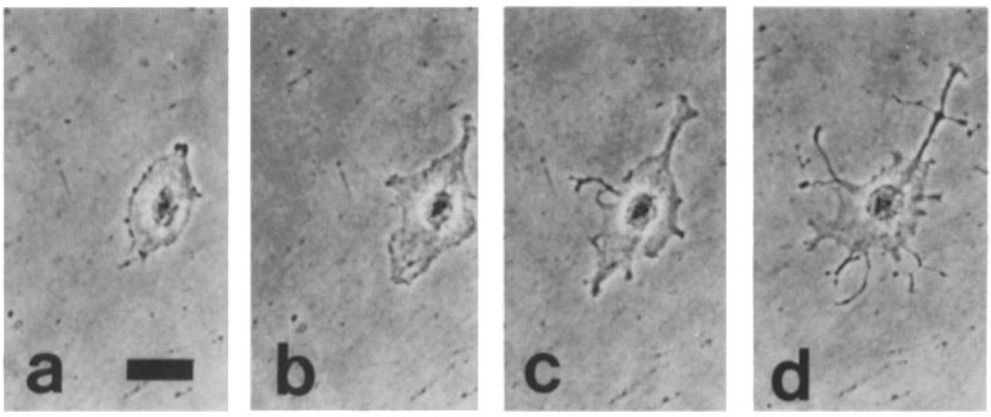

Figure 1. Time lapse photomicrograph of an astrocyte growing processes in response to 1 mM dBcAMP. (*a*) Just before treatment, astrocyte has been allowed to spread on the tissue culture plastic. (*b*) 20 min after addition of dBcAMP, processes emerge. (*C*) 80 min after treatment, processes continue to grow. (*d*) 180 min after treatment. Bar, 50 μm.

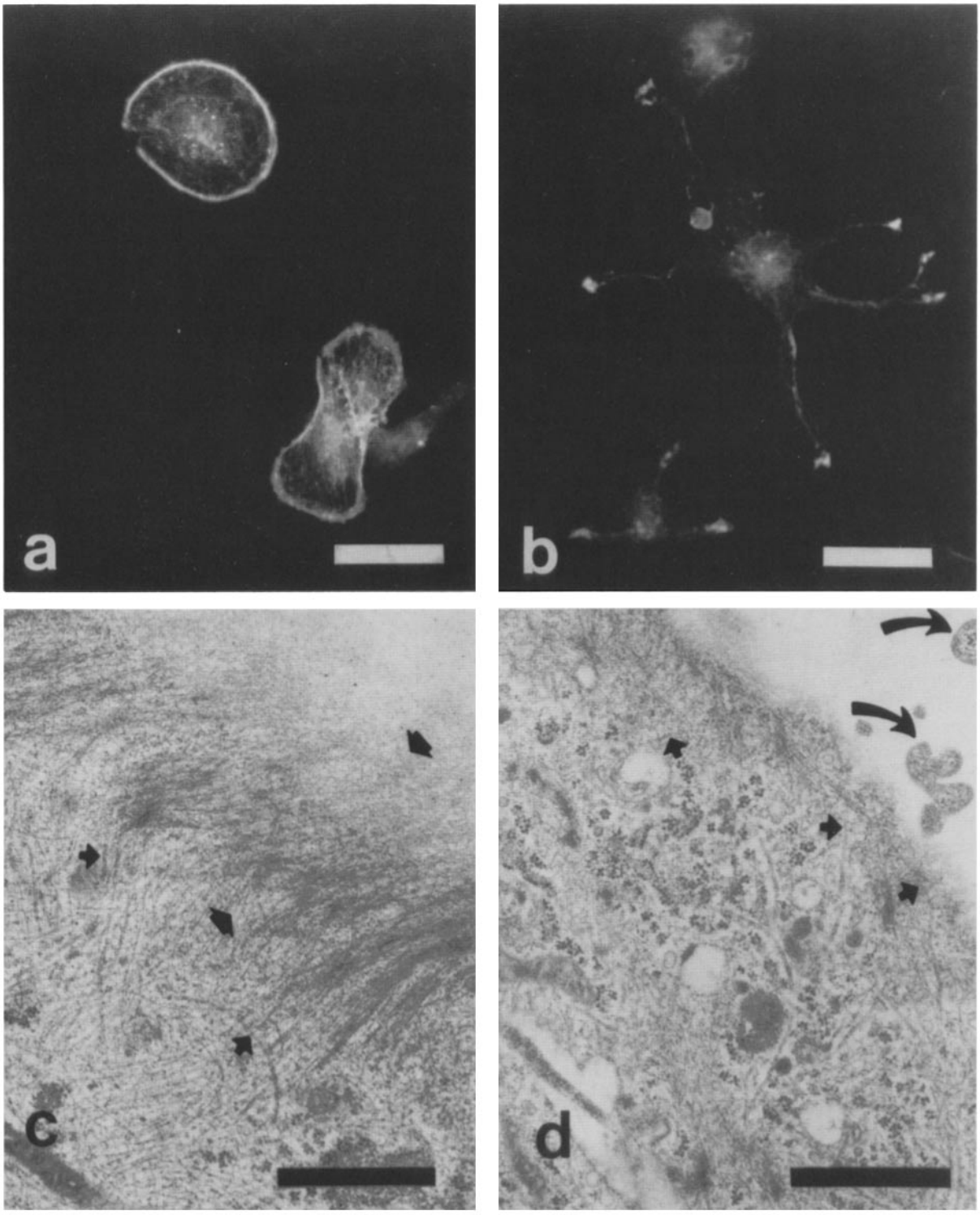

Figure 2. Rearrangement of the cortical actin filament system upon treatment with dBcAMP. (*a*) Astrocytes plated for 180 min without treatment and stained with an antibody to actin. Note prominent cortical staining. (*b*) Astrocytes plated for 180 min in the presence of dBcAMP. Note the absence of the cortical actin filament staining and the appearance of actin staining at the tips of the processes. (*c*) Electron micrograph (*EM*) of an untreated astrocyte plated for 180 min. Note the dense filamentous region at the cell periphery between the two small arrows. (*d*) EM of an astrocyte plated for 180 min in the presence of dBcAMP. Note that the dense cortical region is not present. Straight arrows in *c* and *d* point to microtubules, and curved arrows point to cross sections of narrow structures that are likely processes. Bars: (*a* and *b*) 25 μm; (*c* and *d*) 1.5 μm.

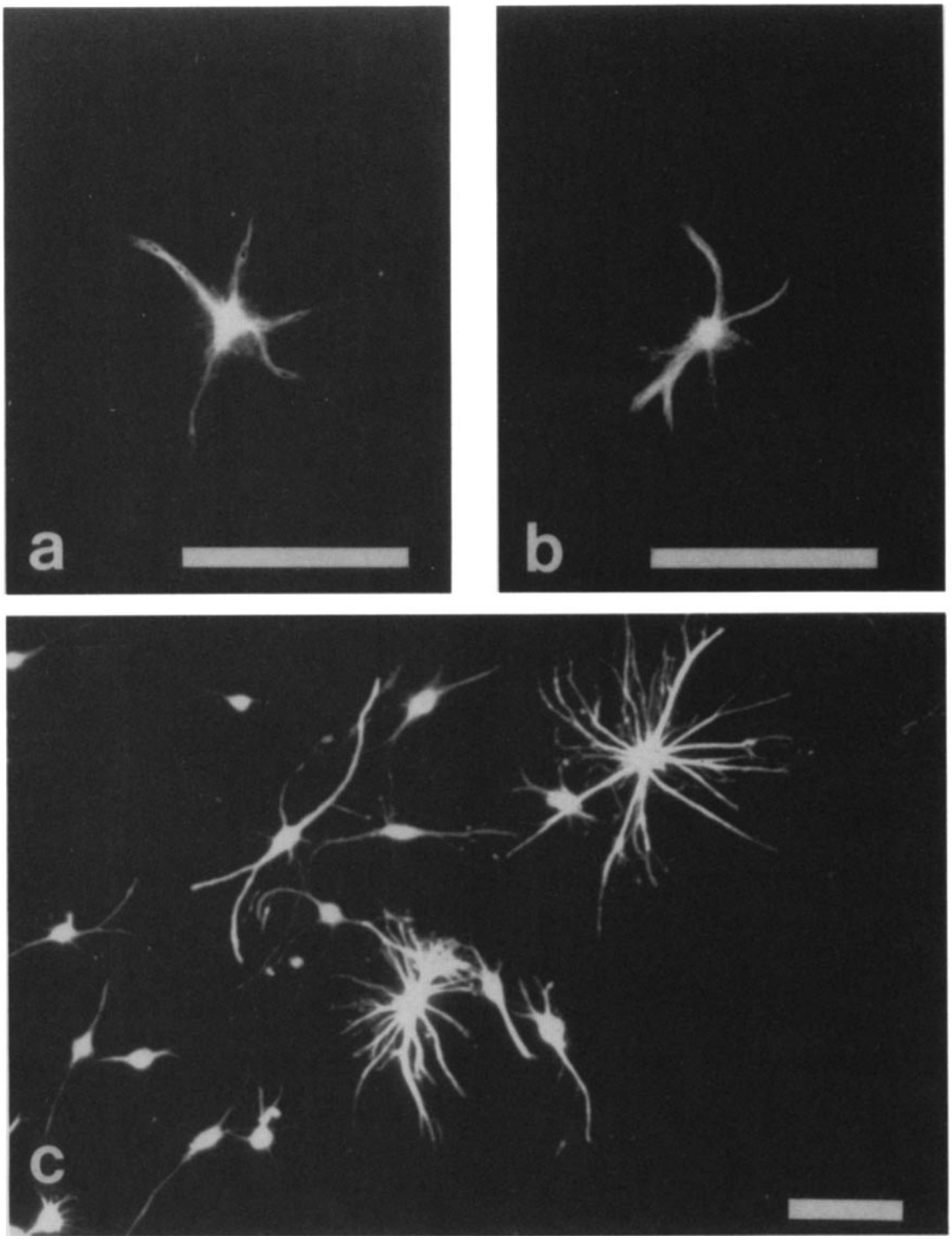

Figure 3. Dihydrocytochalasin B causes the growth of processes similar to dBcAMP. (*a*) Astrocyte plated in the presence of dBcAMP for 80 min and stained for GFAP. (*b*) Astrocyte plated in the presence of dihydrocytochalasin B for 80 min. Note the similarities in the morphologies of the dBcAMP- and dihydrocytochalasin B–treated cells. (*c*) Lower power image of astrocytes treated with dihydrocytochalasin B for 1 d and stained for GFAP. The morphologies induced by dihydrocytochalasin B include bipolar as well as multipolar cells, reflecting a natural distribution of astrocytic morphologies (Mason et al., 1988). Bars, 50 μm.

medium (Fig. 3 *b*). The processes that grow from cells treated at the time of plating are fewer in number and thicker than those formed by cytoplasmic retraction of spread cells treated with dihydrocytochalasin B. Both the caliber and length of the processes that grow from astrocytes treated with dBcAMP or dihydrocytochalasin B at the time of adhesion are similar (Fig. 3, *a* and *b*). The dihydrocytochalasin B-induced processes continue to elongate and by 3 h are

nearly as long as processes grown from cells plated in the presence of dBcAMP. After 24 h in dihydrocytochalasin B, very long processes are seen and some cells have attained stellate morphologies (Fig. 3 *c*). Cotreatment of astrocytes with dBcAMP and dihydrocytochalasin B is indistinguishable from treatment with dihydrocytochalasin B alone. The presence of 10 μM nocodazole prevents the formation of dihydrocytochalasin B–induced processes.

Decrease in Phosphorylation of Myosin Light Chain and Actin Depolymerizing Factor in Cells Treated with dBcAMP

To determine the mechanism of actin filament disruption in astrocytes stimulated with dBcAMP, we examined changes in phosphate incorporation into astrocytic proteins. Only a small number of changes in phosphorylated bands were observed. dBcAMP caused increases in phosphorylation in two bands of molecular weights 51 and 57 kD in the Triton-insoluble fraction. The changes in the phosphorylation of these two Triton-insoluble proteins have been previously reported and the bands have been identified as GFAP and vimentin, respectively (Pollenz and McCarthy, 1986; McCarthy et al., 1985). The morphological differentiation of astrocytes has been dissociated from the phosphorylation of these two proteins (Pollenz and McCarthy, 1986). The other change seen in autoradiograms of Triton-soluble and -insoluble fractions of ^{32}P-labeled cells was a dBcAMP-induced decrease in the ^{32}P phosphate content of bands migrating at 19–20 kD in the Triton-soluble fraction.

Two proteins in the 19–20 kD molecular weight that are known to be involved in regulating microfilaments are the 20-kD regulatory light chain of myosin (MLC) and the 19-kD ADF or destrin (Lamb et al., 1988; Bamburg et al., 1991). We immunoprecipitated these proteins from cells that had been labeled with ^{32}P orthophosphate for 3 h, then treated for 30 min with 1 mM dBcAMP in the continued presence of label. The immunoprecipitation of the myosin complex in untreated cells or cells treated with dBcAMP is shown in Fig. 4. Densitometric scanning of autoradiograms from three experiments showed that there is a 70% decrease in ^{32}P phosphate content in the 20-kD regulatory light chain of myosin after dBcAMP treatment. Inconsistent changes were also seen in a band migrating at the top of these gels. No change could be observed in the total protein as determined by silver stain.

Antibody to ADF was used to immunoprecipitate it from labeled cell extracts either treated or untreated with dBcAMP. The result, shown in Fig. 5 *a*, is that the intensity of the phosphorylated ADF band is decreased 57 ± 6%.

The decreased phosphorylation of the MLC is known to relax actin-dependent tension in smooth muscle cells. To determine whether the decrease in phosphorylation of the myosin light chain and actin depolymerizing factor can be correlated with changes in the tension exerted by actin filaments in astrocytes, we cultured the astrocytes on a thin layer of polymerized silicon fluid. This substrate exhibits visible wrinkles in response to actin-dependent forces exerted by single cells (Harris et al., 1980; Harris, et al., 1981). Fig. 6 (*a* and *c*) shows two fields of astrocytes plated on this substrate, with tension exerted by the astrocyte manifest as wrinkles of the substrate (*arrows*). Note that within 10 min after treatment with dBcAMP (Fig. 6, *b* and *d*), and before a morphological change occurs, the tension exerted by the same astrocytes on the substrate is greatly reduced.

Pharmacological Inhibition of the Myosin Light Chain Kinase Causes Astrocyte Process Growth

The decrease in MLC phosphorylation is consistent with cAMP inhibition of MCL kinase (MLCK). To test this directly, three different inhibitors of MLCK were used. Since MLCK is dependent on calcium-calmodulin for its activity, astrocytes were treated with the calmodulin antagonist, W-7. This treatment induced the formation of processes (Fig. 7 *b*). We also used two selective MLCK inhibitors, ML-9 and KT5926. ML-9 caused the formation of processes at a minimal concentration of 25 μM (Fig. 7 *c*). KT5926 caused the formation of processes at a minimal con-

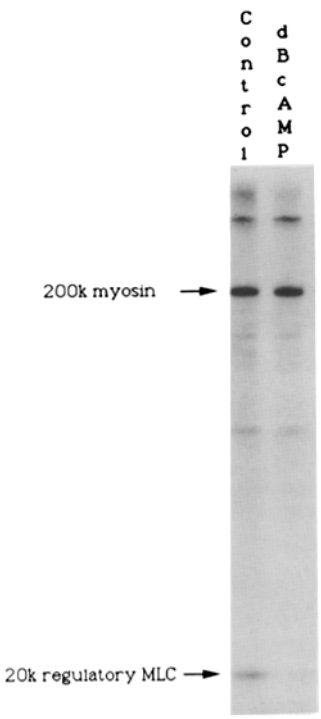

Figure 4. Immunoprecipitation of the myosin complex from astrocytes. A 30-min treatment with dBcAMP causes a significant decrease in the phosphate content of the 20-kD light chain of myosin, while the phosphate content of the 200-kD band remained unchanged. Identity of the other bands in this immunoprecipitate is unknown.

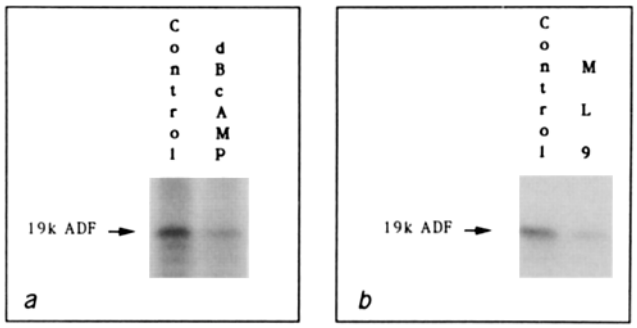

Figure 5. Immunoprecipitation of ADF in astrocytes. (*a*) Decrease in phosphate incorporated into ADF after a 30-min treatment with dBcAMP, run on a 15% PAGE gel. (*b*) Decrease in phosphate incorporated into ADF after a 30-min treatment with 60 μm ML-9.

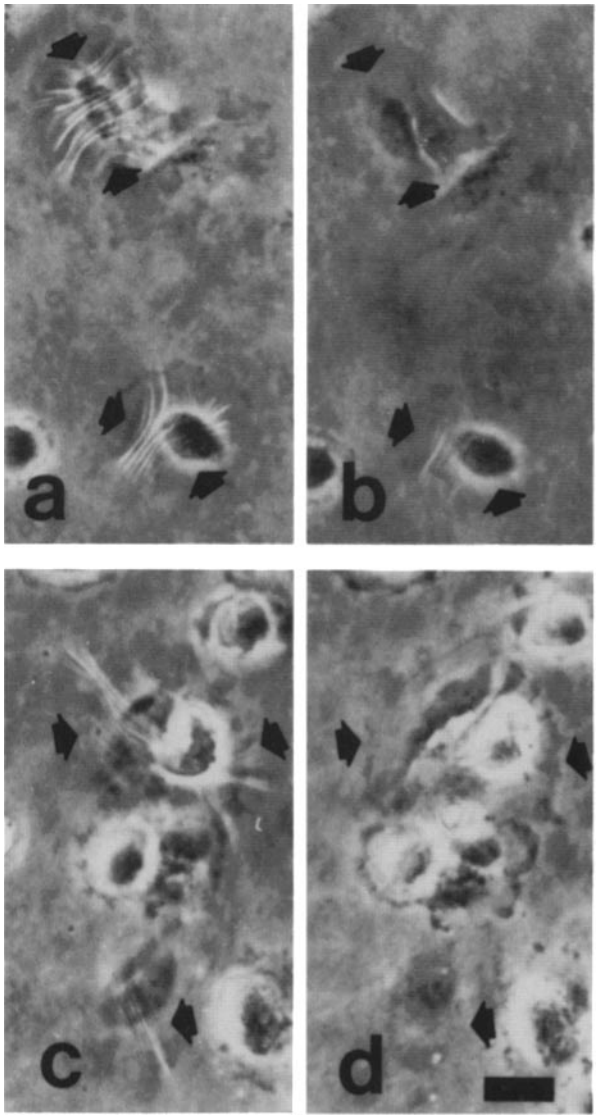

Figure 6. dBcAMP-induced decrease in contractile forces exerted by astrocytes on a silicon substrate. *a* and *c* show two fields of astrocytes contracting the silicon membrane to create wrinkles (*arrows*). *b* and *d* show the same two fields 10 min after the addition of dBcAMP. Note the near elimination of all wrinkles, demonstrating the direct functional consequence of the effect of cAMP on the actin filament system. Bar, 50 μm.

centration of 5 μM. In all three cases, the kinetics of process formation were similar to those seen with cAMP treatment. When ML-9 and KT5926 were removed from the cultures after process formation, the stellate phenotype was preserved for several hours after which they reverted to a polygonal morphology. After 12 h the effect of these drugs was completely reversed. The concentration of KT5926 required to form processes (5–10 μm) is identical to the minimum concentration required to cause a decrease in MLC phosphorylation in rabbit platelets (Nakanishi et al., 1990). The concentration of ML-9 required to cause processes (25 μm) is less than sevenfold its K_i value for the MLCK and well below its K_i for other kinases tested (Saitoh et al., 1986). DMSO had no effect on the morphology of astrocytes at any of the concentrations at which it was used as a vehicle. ML-9 causes the expected decrease in phosphate incorporated into MLC at both concentrations tested (25 and 60 μm) (Fig. 8). A similar decrease is seen with KT5926. Separation of phosphopeptides from immunoprecipitated MLC shows a selective dephosphorylation of the MLCK phosphorylation site without alteration of protein kinase C sites (Fig. 9). ML-9 causes a rapid decrease in phosphate incorporation into ADF as well as MLC (Fig. 5 *b*). ML-9 and KT5926 both cause disruption of filamentous actin. Treatment of astrocytes with 25 μm ML-9 for 3 h causes most of the filamentous actin staining to disappear with some segments of cortical staining remaining and, similar to dBcAMP, filamentous actin is often seen at the tips of the processes (Fig. 10).

Discussion

Disruption of Actin Filaments Leads to the Growth of Astrocytic Processes

Our results show that the physical disruption of the actin filaments in the cell cortex is sufficient to induce process formation. This actin-rich cell cortex normally confers rigidity on the cell membrane. For example, the cortex of a fibroblast is 600-fold stiffer than a lipid bilayer (calculated from data presented by Bray et al., 1986). It is possible that the assembly of microtubules is counterbalanced by the cell cortex which acts as a physical barrier to this growth. Process formation can be viewed as "spring-loaded", requiring only disassembly of cortical F-actin to relieve the constraint on growth.

The prevention of process elongation by nocodazole indicates that the "spring" in this system is microtubule dependent. The evidence that particles larger than 7 nm cannot penetrate into actin filament structures such as stress fibers and the leading edge of fibroblasts (Luby-Phelps and Taylor, 1988; Luby-Phelps et al., 1987; Luby-Phelps et al., 1986) is consistent with the concept that structures as large as microtubules (25 nm) cannot assemble in regions rich in actin filaments because the three-dimensional mesh is too small. Microtubule assembly and organelle movement to form polarized structures such as astrocyte processes would then require the disruption of filamentous actin. The physiological disruption of actin filaments accompanying morphogenesis occurs in several systems. Cytochalasin B has been shown to cause an arborization of fibroblasts, a morphological change that was proposed to be dependent on intermediate filaments (Menko et al., 1983; Croop and Holtzer, 1975). In another case, the elongation of retinal photoreceptor cells was proposed to be controlled by opposing microtubule and actin-dependent forces, where actin filaments create forces that resist photoreceptor elongation, while the elongating force is dependent on microtubules (Madreperla and Adler, 1989). In this case, cytochalasin D causes an increase of photoreceptor length within hours. Another example is the neuronal growth cone, where the most distal portion is rich in filamentous actin, while microtubules and organelles are normally restricted to the neurite shaft and proximal portion of the growth cone. The normal advance of microtubules and organelles into the distal portion of the growth cone, called engorgement, can be rapidly stimulated by disrupting actin filaments with cytochalasin B (Goldberg

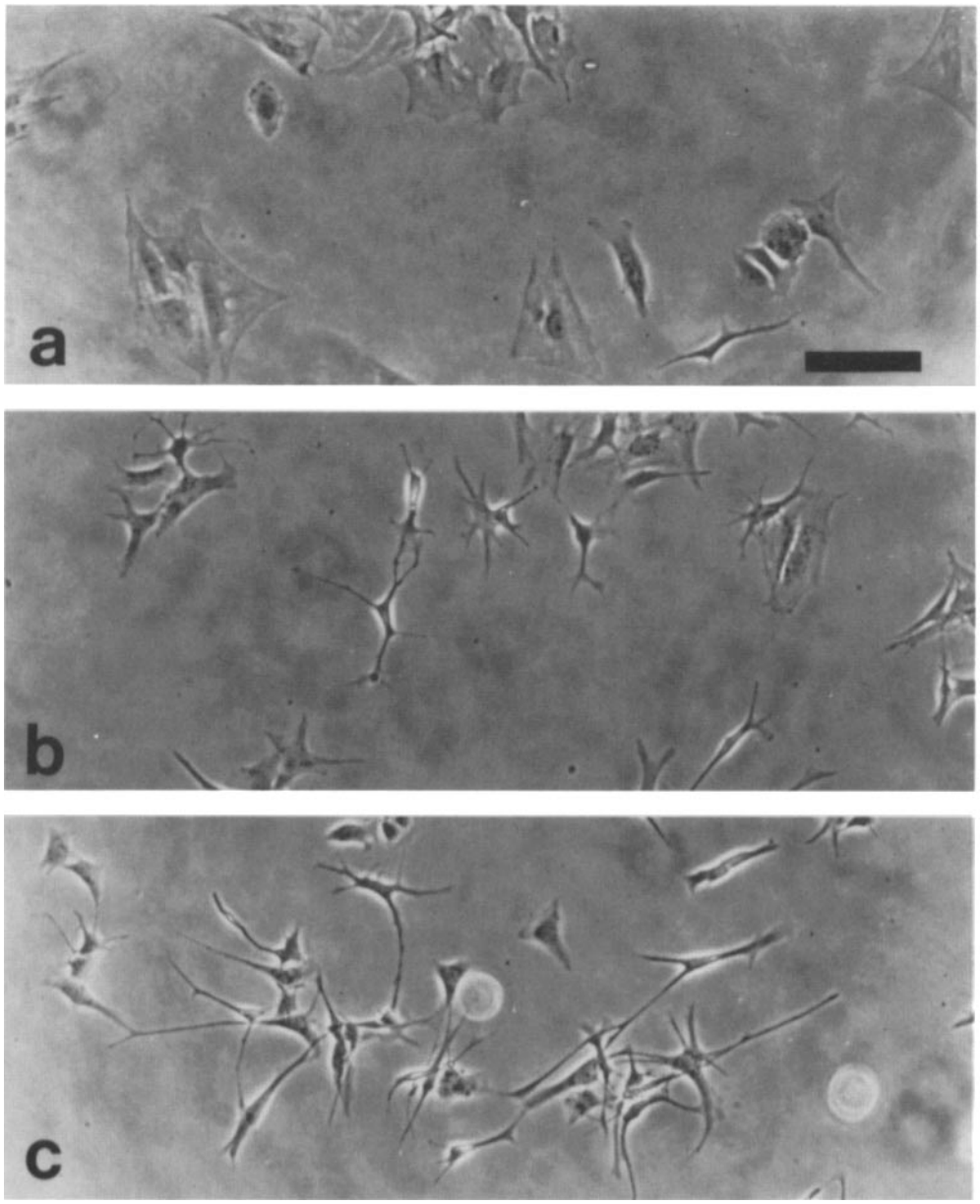

Figure 7. Inhibition of the MLCK causes process formation in astrocytes. (*a*) Control cells plated in medium containing 3% serum for 9 h. (*b*) Presence of 50 μm W-7 causes the formation of processes, as does 25 μm ML-9 (*c*). Bar, 100 μm.

and Burmeister, 1989; Burmeister et al., 1991; Forscher and Smith, 1988). This supports the idea that physiologic disruption of filamentous actin may promote elongation by allowing the distal invasion of microtubules and organelles (Bray, 1987; Burmeister et al., 1991; Forscher and Smith, 1988).

Although the hypothesis that actin filaments play the role of an impenetrable cortical barrier is an attractive one, it may be an oversimplification. It is possible, for example, that the critical result of actin filament breakage is the release of cellular attachments to the substrate. Treatment of astrocytes with dBcAMP causes the disappearance of vinculin-containing attachment sites (Goldman and Abramson, 1990). While the release of certain attachment sites may be involved in the growth of processes, it is clear that breaking the actin cortical barrier is necessary.

The actin rearrangement seen in response to dBcAMP involves not only dispersal of all filamentous actin in the cell cortex, but the appearance of actin filaments at the tips of the processes. The role actin plays at the leading edge is not required for process formation since dihydrocytochalasin B causes elongation of processes without the actin filaments at the tip. However, in the presence of dihydrocytochalasin D the growing tip is blunt and does not show the formation of filopodia and lamellipodia present on dBcAMP treatment. These actin-dependent events are likely to be important in modifying or guiding process growth in a manner analogous to the neuronal growth cone.

The Decrease in Phosphorylation of MLC and ADF Can Affect Actin Filament Integrity

The phosphorylation state of MLC controls the interaction between actin and myosin in smooth muscle cells (Mrwa and Hartshorne, 1980). Phosphorylation of the regulatory MLC

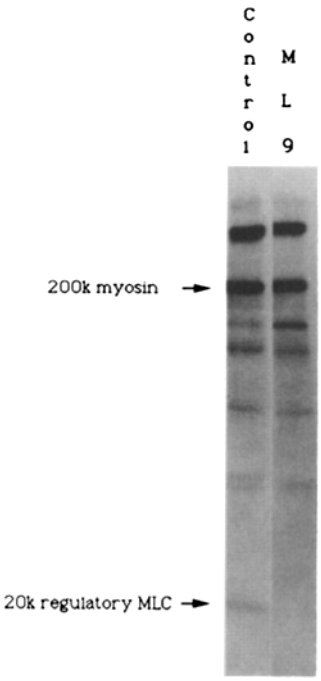

Figure 8. Immunoprecipitation of the myosin complex from astrocytes either untreated (*Control* lane) or treated with 60 μm ML-9 for 1 h (*ML-9* lane). Samples run on a 6–12% gradient gel.

exposes the actin binding site on the myosin head permitting actin to activate the Mg^{+2}-ATPase activity of myosin and causing contraction. MLC phosphorylation also frees the myosin tail to interact with other myosin tails and form a myosin filament. Decreasing the phosphorylation of MLC reverses these effects, causing relaxation of tension developed between actin and myosin filaments, and resulting in destabilization of myosin filaments which could lead to a weakening of actin filament networks. It is possible that the decreased phosphorylation of MLC alone is sufficient to cause destabilization of actin filaments (Lamb et al., 1988). We have demonstrated that the cAMP-induced decrease in phosphorylation of the astrocytic MLC correlates with a reduction in the contractile forces exerted by cell on silicon substrates much as it does in smooth muscle and that the observed alterations in actin filament distribution reflect a reduction of tension in the cell cortex.

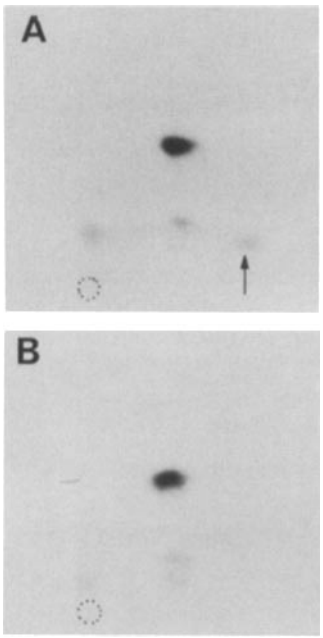

Figure 9. Separation of phosphopeptides from immunoprecipitated myosin light chain after orthophosphate labeling. Electrophoresis from left to right and chromotography from bottom to top. (*A*) Control cells. Arrow points to MLCK phosphorylated site (serine 19). (*B*) ML-9–treated cells. Note inhibition of labeling in serine 19 containing phosphopeptide.

The other protein examined in this study, ADF, is a 19-kD protein that was initially purified from embryonic chick brain (Giuliano et al., 1988). ADF is present in mammalian brain and cultured cell lines, particularly at the leading edge of ruffled membranes and in the neuronal growth cone (Bamburg and Bray, 1987). This protein has the ability to bind actin monomers and to sever existing actin filaments (Giuliano et al., 1988). A 19-kD porcine protein that shares 95% sequence homology with chick ADF as well as identical actin depolymerizing activity has been called destrin (Moriyama et al., 1990; Nishida et al., 1984; Bamburg et al., 1991). The treatments that decreased the phosphorylation of MLC in our study (dBcAMP and ML-9) also decreased the phosphorylation of ADF though it is likely that this is not a direct action of MLCK on ADF. Phosphorylated ADF has been found to be inactive in severing actin filaments, indicating that the decrease in phosphorylation we see may represent activation of the actin-severing activity of this protein in the cell. Although the relative contributions of MLC and ADF to process initiation have not been assessed, the dephosphorylation of either or both could lead to the disruption of microfilaments. It is likely that both of these systems work together to release tension and break down filamentous actin. Decreased phosphorylation of MLC could relieve tension exerted between actin and myosin, and destabilize myosin filaments, which might then make actin filaments more accessible to the subsequent severing activity of ADF. An interesting possibility is that the phosphorylation of MLC also favors a shift of actin interactions from myosin 2 to myosin 1 and that the actin filaments seen at the growing tips could be associated with myosin 1 molecules.

In spite of the dramatic morphological alterations in cortical actin, we have seen only a modest shift of actin from F-actin to the soluble pool. Other workers (Goldman and Abramson, 1990) have seen shifts as great as 40%. This difference may be due in part to the far greater number of stress fibers, which break down in response to dBcAMP, in their cultures. In either case, it is clear that only a portion of the F-actin solubilized during process formation. There is also a shift of F-actin to the tips of the growing processes. ADF is an actin monomer binding protein as well as an actin filament severing protein, so that in addition to severing, it may serve to control actin filaments by binding soluble actin.

The MLCK as a Control Switch

The phosphorylation of MLC can be controlled by regulating the activity of the myosin light chain kinase. This enzyme is a calcium-dependent kinase (Sherry et al., 1978) that requires the binding of the calcium–calmodulin complex for its activity. Phosphorylation of MLCK by the cAMP-dependent kinase reduces its affinity for calcium–calmodulin, and thus lowers the rate at which it phosphorylates MLC (Conti and Adelstein, 1980).

Inhibition of MLCK by the MLCK-selective kinase inhibitor, ML-9, supports the notion that the inhibition of MLCK is sufficient to cause a decreased phosphorylation of the MLC. However, ML-9 also leads to a decrease in ADF phos-

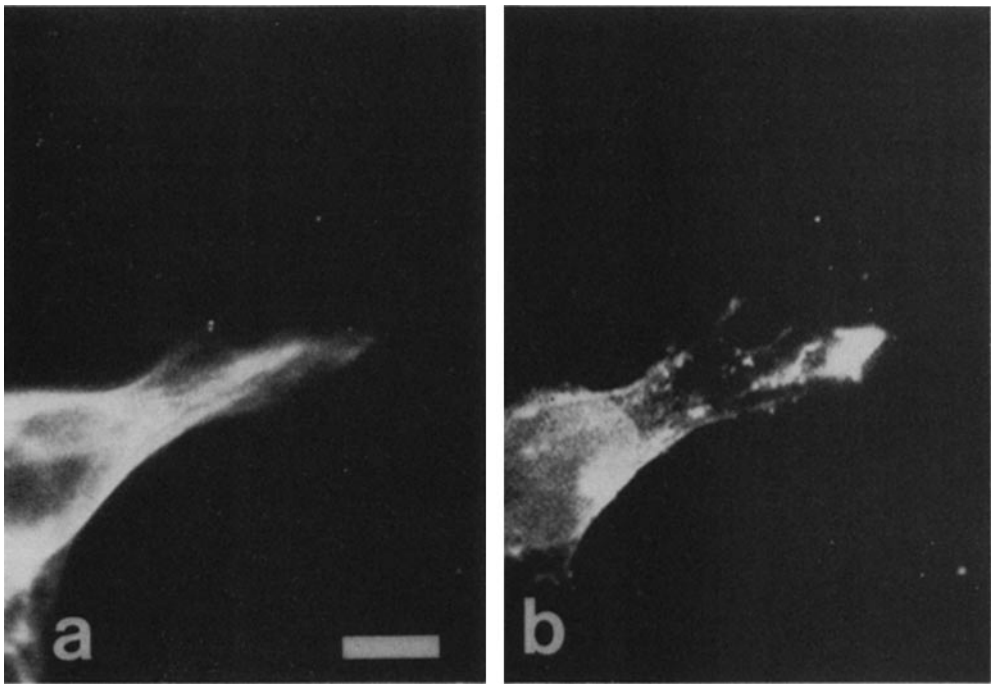

Figure 10. GFAP stain (*a*) and corresponding actin stain (*b*) in a cell treated with 25 μm ML-9 for 3 h. Note the actin staining at the tips of the processes as was seen in cells treated with dBcAMP. Bars, 50 μm.

phorylation. It is possible that ADF is normally a target of MLCK, and that ML-9 directly blocks the phosphorylation of ADF by inhibiting MLCK. Alternatively, steric changes in the actin filament system caused by ML-9's effect on MLC phosphorylation could make ADF less accessible to another kinase. ML-9 and KT5926 were previously found to be highly selective for MLCK as compared to other kinases tested and in this study were used at concentrations consistent with their selective inhibition of MLCK (Saitoh et al., 1986; Nakanishi et al., 1990). Our work shows no detectable changes in phosphorylation of any proteins other than MLC and ADF in cells treated with ML-9.

Conclusion

Our findings suggest that process formation in astrocytes is the direct result of the breakdown of the cortical actin web and that this is controlled by the regulation of the phosphorylation of MLC and ADF by the MLCK. These findings place the control of morphogenesis in the realm of smooth muscle biochemistry and its interaction with microtubule assembly. It is probable that this is a general mechanism that is modified in various cell types by substitution of other actin severing proteins for ADF and by variations in the pathways for regulation of the activity of MLCK.

We thank Drs. Robert Adelstein, James Bamburg, Ron Liem, and Chloe Bulinski for use of their antibodies, and Ron Liem, James Goldman, David Colman, and Carol Mason for their helpful criticism over the course of this work.

This work was supported by grant number NS15076 from the National Institutes of Health.

Received for publication 17 September 1991 and in revised form 31 January 1992.

References

Adelstein, R. S. 1980. Phosphorylation of muscle contractile proteins. *Fed. Proc.* 39(5):1544–1546.

Bamburg, J. R., and D. Bray. 1987. Distribution and cellular localization of actin depolymerizing factor. *J. Cell Biol.* 105:2817–2825.

Bamburg, J. R., L. S. Minamide, T. E. Morgan, S. M. Hayden, K. A. Giuliano, and A. Koffer. 1991. Purification and characterization of low-molecular weight actin-depolymerizing proteins from brain and cultured cells. *Methods Enzymol.* 196:125–140.

Bray, D. 1987. Growth cones: do they pull or are they pushed? *TINS (Trends Neurosci).* 10(10):431–434.

Bray, D., J. Heath, and D. Moss. 1986. The membrane-associated 'cortex' of animal cells: its structure and mechanical properties. *J. Cell Sci. Suppl.* 4:71–88.

Burmeister, D. W., R. J. Rivas, and D. J. Goldberg. 1991. Substrate bound factors stimulate engorgement of growth cone lamellipodia during neurite elongation. *Cell Mot. Cytoskeleton.* 19:255–268.

Conti, M. A., and R. S. Adelstein. 1980. Phosphorylation by cyclic 3′:5′-monophosphate-dependent protein kinase regulates myosin light chain kinase. *Fed. Proc.* 39(5):1569–1573.

Cornell-Bell, A. H., S. M. Finkbeiner, M. S. Cooper, and S. J. Smith. 1990. Glutamate induces calcium waves in cultured astrocytes: long-range glial signaling. *Science (Wash. DC).* 247:470–473.

Croop, J., and H. Holtzer. 1975. Response of myogenic and fibrogenic cells to cytochalasin B and to colcemid. *J. Cell Biol.* 65:271–285.

Forscher, P., and S. J. Smith. 1988. Actions of cytochalasins on the organization of actin filaments and microtubules in a neuronal growth cone. *J. Cell Biol.* 107:1505–1516.

Giuliano, K. A., F. A. Khatib, S. M. Hayden, E. W. R. Daoud, M. E. Adams, D. A. Amorese, B. W. Bernstein, and J. R. Bamburg. 1988. Properties of purified actin depolymerizing factor from chick brain. *Biochemistry.* 27(25): 8931–8938.

Goldberg, D. J., and D. W. Burmeister. 1989. Looking into growth cones. *TINS (Trends Neurosci.)* 12(12):503–506.

Goldman, J. E., and B. Abramson. 1990. Cyclic AMP-induced shape changes of astrocytes are accompanied by rapid depolymerization of actin. *Brain Res.* 528:189–196.

Goldman, J. E., and F. Chiu. 1984. Dibutyryl cyclic AMP causes intermediate filament accumulation and actin reorganization in astrocytes. *Brain Res.* 306: 85–95.

Harris, A. K., P. Wild, and D. Stopak. 1980. Silicon rubber substrata: a new wrinkle in the study of cell locomotion. *Science (Wash. DC).* 208:177–179.

Harris, A. K., D. Stopak, and P. Wild. 1981. Fibroblast traction as a mechanism for collagen morphogenesis. *Nature (Lond.).* 290:249–251.

Hatten, M. E. 1985. Neuronal regulation of astroglial morphology and proliferation in vitro. *J. Cell Biol.* 100:384–396.

Kimelberg, H. K., and M. D. Norenberg. 1989. Astrocytes. *Scientific American.* April, 1989. 260:66–76.

Laemmli, U. K. 1970. Cleavage of structural proteins during the assembly of the head of bacteriophage T4. *Nature (Lond.).* 227:680–685.

Lamb, N. J. C., A. Fernandez, M. A. Conti, R. Adelstein, D. B. Glass, W. J.

Welch, and J. R. Feramisco. 1988. Regulation of actin microfilament integrity in living cells by the cAMP-dependent protein kinase and the myosin light chain kinase. *J. Cell Biol.* 106:1955–1971.

Lim, R., K. Mitsunobu, and W. K. P. Li. 1973. Maturation-stimulating effect of brain extract and dibutyryl cyclic AMP on dissociated embryonic brain cells in culture. *Exp. Cell Res.* 79:243–247.

Luby-Phelps, K., and D. L. Taylor. 1988. Subcellular compartmentalization by local differentiation of cytoplasmic structure. *Cell Motil. Cytoskeleton.* 10:28–37.

Luby-Phelps, K., D. L. Taylor, and F. Lanni. 1986. Probing the structure of cytoplasm. *J. Cell Biol.* 102:2015–2022.

Luby-Phelps, K., P. E. Castle, D. L. Taylor, and F. Lanni. 1987. Hindered diffusion of inert tracer particles in the cytoplasm of mouse 3T3 cells. *Proc. Natl. Acad. Sci. USA.* 84:4910–4913.

Ludowyke, R. I., I. Peleg, M. A. Beaven, and R. S. Adelstein. 1989. Antigen-induced secretion of histamine and the phosphorylation of myosin by protein kinase C in rat basophilic leukemia cells. *J. Biol. Chem.* 264(21):12492–12501.

Madreperla, S. A., and R. Adler. 1989. Opposing microtubule- and actin-dependent forces in the development of structural polarity in retinal photoreceptors. *Dev. Biol.* 131:149–160.

Mason, C. A., J. C. Edmondson, and M. E. Hatten. 1988. The extending astroglial process: development of glial shape, the growing tip, and interactions with neurons. *J. Neurosci.* 8(9):3124–3134.

McCarthy, K. D., and J. de Vellis. 1978. Alpha-adrenergic receptor modulation of beta-adrenergic adenosine and prostaglandin E1 increased adenosine 3′:5′-cyclic monophosphate levels in primary cultures of glia. *J. Cyclic Nucleotide Res.* 4:15–26.

McCarthy, K. D., J. Prime, T. Harmon, and R. Pollenz. 1985. Receptor-mediated phosphorylation of astroglial intermediate filament proteins in cultured astroglia. *J. Neurochem.* 44(3):723–730.

Menko, A. S., Y. Toyama, D. Boettiger, and H. Holtzer. 1983. Altered cell spreading in cytochalasin B: a possible role for intermediate filaments. *Mol. Cell. Biol.* 3(1):113–125.

Moriyama, K., E. Nishida, N. Yonezawa, H. Sakai, S. Matsumoto, K. Iida, and I. Yahara. 1990. Destrin, a mammalian actin-depolymerizing protein, is closely related to cofilin. *J. Biol. Chem.* 265(10):5768–5773.

Mrwa, U., and D. J. Hartshorne. 1980. Phosphorylation of smooth muscle myosin and myosin light chains. *Fed. Proc.* 39:1564–1568.

Murphy, S., and B. Pearce. 1987. Functional receptors for neurotransmitters on astroglial cells. *Neuroscience.* 22(2):381–394.

Nakanishi, S., K. Yamada, K. Iwahashi, K. Kuroda, and H. Kase. 1990. KT5926, a potent and selective inhibitor of myosin light chain kinase. *Mol. Pharmacol.* 37:482–488.

Nishida, E., S. Maekawa, E. Muneyuki, and H. Sakai. 1984. Action of a 19k protein from porcine brain on actin polymerization: a new functional class of actin-binding proteins. *J. Biochem.* 95:387–398.

Nishikawa, M., H. Hidaka, and R. S. Adelstein. 1983. Phosphorylation of smooth muscle heavy meromyosin by calcium-activated, phospholipid-dependent protein kinase. *J. Biol. Chem.* 258:14069–14072.

Pollenz, R. S., and K. D. McCarthy. 1986. Analysis of cyclic AMP-dependent changes in intermediate filament protein phosphorylation and cell morphology in cultured astroglia. *J. Neurochem.* 47(1):9–17.

Saitoh, M., M. Naka, and H. Hidaka. 1986. The modulatory role of myosin light chain phosphorylation in human platelet activation. *Biochem. Biophys. Res. Commun.* 140(1):280–287.

Shain, W., D. S. Forman, V. Madelian, and J. N. Turner. 1987. Morphology of astroglial cells is controlled by beta-adrenergic receptors. *J. Cell Biol.* 105:2307–2314.

Sherry, J. M. F., A. Gorecka, M. O. Aksoy, R. Dabrowska, and D. J. Hartshorne. 1978. Roles of calcium and phosphorylation in the regulation of the activity of gizzard myosin. *Biochemistry.* 17(21):4411–4418.

Stossel, T. P. 1984. Contribution of actin to the structure of the cytoplasmic matrix. *J. Cell Biol.* 99:15s–21s.

Towbin, H., T. Staehelin, and J. Gordon. 1979. Electrophoretic transfer of proteins from polyacrylamide gels to nitrocellulose sheets: procedure and some applications. *Proc. Natl. Acad. Sci. USA.* 76(9):4350–4354.

Trimmer, P. A., P. J. Reier, T. H. Oh, and L. F. Eng. 1982. An ultrastructural and immunocytochemical study of astrocytic differentiation in vitro. *J. Neuroimmunol.* 2:235–260.

Walz, W. 1989. Role of glial cells in the regulation of the brain microenvironment. *Prog. Neurobiol.* 33:309–333.

Wray, W., T. Boulikas, V. P. Wray, and R. Hancock. 1981. Silver staining proteins in polyacrylamide gels. *Anal. Biochem.* 118:197–203.